Removal of Heavy Metals from Aqueous Solution by Mordenite Nanocrystals

A. Pourahmad[1*], Sh. Sohrabnezhad[2], B. Sadeghi[3]

1- Department of Chemistry, Faculty of Science, Islamic Azad University, Rasht Branch, Rasht, I. R. Iran
2- Department of Chemistry, Faculty of Science, University of Mohaghegh Ardabili, Ardabil, I. R. Iran
3- Department of Chemistry, Faculty of Science, Islamic Azad University, Tonekabon Branch, I. R. Iran

(*) Corresponding author: pourahmad@iaurasht.ac.ir
(Received: 30 Nov. 2009 and Accepted: 01 Mar. 2010)

Abstract:

This study examined the ability of the synthetic mordenite nanocrystal to remove Tl(III) and As(III) from an aqueous solution. The determination of the concentration changes of H^+ and OH^- quantities in the acidic (pH 3) and alkali (pH 9) treated mordenite nanocrystals were done by the potentiometric titration curves. The maximum uptake capacities (Q_{max}) of these metal ions using the mordenite in the separate batch reactors from 278 to 323 K were obtained about 0.627-0.836 and 0.563-0.742 mmol/g, for Tl(III) and As(III), respectively. In order to remove these metal ions, the enthalpy change (ΔH) was 11.236 and 9.856 kJ/mol and the entropy change (ΔS) was 38.1 and 42.9 J/mol K, respectively. Mordenite nanocrystal removed these heavy metals corresponding to pseudo-second-order kinetic model.

Keywords: *Mordenite nanocrystal; Heavy metals; Adsorption kinetics; Wastewater treatment*

1. INTRODUCTION

The different methods are used for the removal of heavy metals as important contaminants in water and wastewater. The chemical methods such as precipitation with lime or caustic soda effectively decrease heavy metals to the acceptable levels which require a large excess of chemicals that generate volumetric sludge and increase the costs [1, 2].

Among various techniques, the adsorption process is exclusively used in water treatment and many studies have been carried out to find inexpensive and chemico-physically feasible adsorbent. Natural and synthetic zeolites have received much attention over the past decades in water treatment due to their unique pore structure and cation-exchange properties. Most of the adsorbents including zeolites, however, present some disadvantages such as poor adsorption capacity, low efficiency based on economic point of view and ineffectiveness for low metal concentrations [3].

The nanometer materials are new functional materials [4], which have attracted much attention due to its special properties. Most of the atoms on the surface of the nanoparticles are unsaturated and can easily bind with the other atoms. Nanoparticles have high adsorption capacity. Besides, the operation is simple, and the adsorption process is rapid. So there is a growing interest in the application of nanoparticles as sorbents [5].

Mordenite is a zeolite with an ideal composition of $Na_8Al_8Si_{40}O_{96}.\ nH_2O$ and a structure refined in the Cmcm space group. The unit cell of sodium

mordenite has dimensions a=18.121ºA, b=20.517ºA, and c=7.544ºA. The most common morphology of mordenite is characterized by needles with c direction elongation. The micropore system of mordenite consists of two pore channels; an elliptical pore channel (6.7×7.0ºA) which runs parallel to the c-axis and, another pore channel which runs parallel to the b-axis (2.6×5.7ºA) [6].

Due to its high thermal and acid stability, mordenite has been used as catalyst for important reactions, such as hydrocracking, hydroisomerization, alkylation, reforming, dewaxing and the production of dimethylamines [7-9]. Mordenite has been also used in the adsorptive separation of gas or liquid mixtures [10]. In addition, mordenite has been considered to be used for applications in semiconductors, chemical sensors, and nonlinear optics [11-13].

Nanosized zeolites are important in catalytic and adsorptive applications. Smaller crystals of zeolites will have larger surface areas and less diffusion limitations compared to zeolites with micrometer-sized crystals [14]. Nanometer-sized zeolites also offer advantages in supramolecular catalysis, photochemistry, nanochemistry, electrochemistry, and optoelectronics [15]. Zeolite nanocrystals can also be used in the construction of other geometries such as thin films, fibers, and self-standing zeolite membranes [16].

In this study, mordenite nanocrystal was used to remove Tl (III) and As (III) from aqueous solution and the experimental conditions were studied and optimized. The thermodynamic and kinetic modeling also was obtained.

2. MATERIALS AND METHODS

2.1. Adsorbent

Nano-sized mordenite zeolites with particle size~90 nm were synthesized by adjusting gel compositions and crystallization conditions in the described procedure in the literature [17]. The chemical composition of the mordenite nanocrystals gels were Al_2O_3: $30SiO_2$: $6Na_2O$: $780H_2O$. Then, the reaction mixture were introduced into a stainless-steel autoclave, heated up to 170ºC and kept for a given time until crystallization was completed. After the autoclave was quenched in cold water, the crystalline products were filtered, washed with water and dried at 110ºC ov er night. Then the samples were calcined in a muffle furnace at 540ºC for 5 h.

2.2. Adsorbent characterization

Powder X-ray diffraction patterns of the samples were recorded using a X'pert diffractometer with Cu Kα radiation (λ=1.54ºA).

The specific surface area and pore volume of the samples were measured using a Sibata Surface Area Apparatus 1100. All of the samples were first degassed at 250ºC for 2 h.

2.3. Batch sorption experiments and equilibrium model

The Tl (III) and As (III) stock solutions were prepared by dissolving their corresponding nitrite salts (analytical grade from Merck) in distilled water, separately and standardized by atomic adsorption spectrophotometry.

For equilibrium studies (to obtain adsorption isotherms), a series of flasks (250 ml, as batch sorption reactors) were prepared containing heavy metal solutions (100 ml) of known concentrations (C_o) varying from 0.53 to 4.20 mM (each solution contained one metal ion). The experiments conditions were as follows: addition of mordenite nanocrystal (200 mg) into each flask (dose 2.0 g adsorbent/ l), agitating mixtures (150 rpm) for10 h as the adsorption time at each of used temperatures viz. 5, 25 and 50°C with changes range of ±0.5°C and adjusting adsorption pH at the optimal values for each metal ions (according to Figure 3) using 0.1M NaOH and 0.1M HCl during the equilibrium period. The mordenite nanocrystal was removed at last by filtration through a 0.45 µm membrane filter (Millipore) and the filtrate was analyzed for ion content (C_e) by atomic absorption spectrophotometry.

The isotherms can be described by Langmuir equation:

$$q_e = Q_{max} K_L C_e/(1+K_L C_e) \quad (1)$$

The Langmuir equation transforms to the linearized form:

$$C_e/q_e = C_e/Q_{max} + 1/(Q_{max}. KL) \quad (2)$$

that Q_{max} and b are found from the slop and intercept of C_e/q_e vs. C_e linear plot such that Q_{max}=1/slope, and b=(slope /intercept). q_e is given from the following relation:

$$q_e = (C_o - C_e)/(m/V) \quad (3)$$

Where: Co is the initial concentration of the metal ions (mM or mg/l), m is the adsorbent dry weight (g) and V is suspension volume (l).

2.4. Sorption pH and blank tests

In this study, the solutions pH for the sorption process adjusted from 1.0 to 8.0, individually, for each metal ion sample (Co=1.00 mM) by 0.2 M HCl and 0.2 M NaOH solutions. The work at the pH values higher than the limits that the metal ions were precipitated get restricted the true sorption studies. So it was used the 0.2 M HCl solutions to dissolve the precipitates to determine the concentration of the unsorbed metal ions. All the sorption experiments were run at the obtained optimal pH values from Figure 3 for each metal ion.

Blank tests: In order to eliminate the ions removal effect in the high pHs by the precipitating as the hydroxide salts, the blank tests were carried out. In these tests, were selected the samples of within cations solution, only (without mordenite) and separately, as blank in the same conditions of the pretreatment experiments. The correction was applied in comparison between the removal values in the blank and experimental solutions for the ions at all studies. Therefore we could determine the cations that are removed only by mordenite nanocrystal easily.

2.5. Sorption time

The contact times of 25 to 200 min were selected for the metal solutions (Co=1.00 mM) with 2.0 g adsorbent/l at the obtained optimal pHs for each metal ion from the previous study. These pH values were almost 8.0 and 6.5 for Tl (III) and As (III) respectively (Figure 3).

2.6. Acid-base and base-acid potentiometric titrations

The treated mordenite nanocrystal samples by 0.1M HCl (at pH 3) and 0.1 M NaOH (at pH 9) after 1 hr, were washed with deionized water, and then the suspensions as 0.2 g of it in 100 ml of solution were potentiometrically titrated with 0.2 M HCl (for the basic pre-treated sample) and 0.2 M NaOH (for the acidic pre-treated sample), separately.

The pH electrode were calibrated with pH 3.00, 6.00 and 9.00 (with range ± 0.01) buffers just before titrations. The initial pH of solutions was adjusted to 7.0 ± 0.05 with 0.01 M HCl and NaOH and the solutions were titrated by a Mettler-Toledo DL 53 titrator (Schwerzenbach, Switzerland). The solutions in the vessel were agitated by a magnetic stirrer (500 rpm) until pH became stable after each titrant aliquot injection. The pH was noted when the value was stable for 100 second.

3. RESULTS AND DISCUSSION

Figure 1 presents the XRD pattern of mordenite nanocrystal zeolite. The XRD profile of mordenite nanocrystal shows quite well with patterns that is given in literatures [14, 17- 19] which allowed up to identify the product as crystalline mordenite zeolite. We have determined the nanoparticles size by using the Debye-Scherrer formula, $d=0.9 \lambda /\beta \cos\theta$, where d is the average diameter of the crystalline, θ is the wavelength of X-ray, β is the excess line width of the diffraction peak in radians and θ is the Bragg angle. Based on this analysis the average size of mordenite nanocrystals have been found to be ~9 nm.

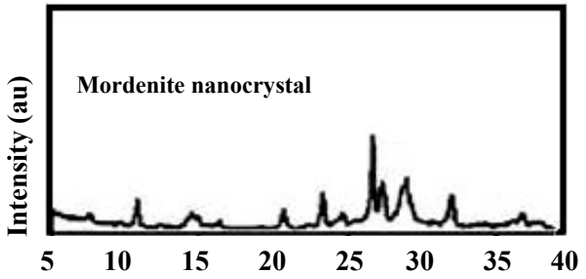

Figure 1: *XRD pattern of mordenite nanocrystal zeolite*

The specific surface area and pore volume of the mordenite and mordenite nanocrystal are presented in Table 1.

It can be seen that mordenite nanocrystal zeolite has a surface area of 379 m^2g^{-1} while the mordenite zeolite only has a surface area of 240 m^2g^{-1} (Table 1). The pore volume of two adsorbents also demonstrates that mordenite nanocrystal is a porous material has a pore volume of 0.18 cm^3g^{-1} with micropores. AlsoIt can be seen that mordenite nanocrystal zeolite has much higher adsorption than mordenite.

The surface morphology of mordenite nanocrystal is investigated by SEM and the micrographs are presented in Figure 2. As can be observed in the SEM image, the powders are constituted by bundles of needle-like crystals. It is known that typically the mordenite crystals are needle-shaped for low Si/Al ratios [20].

Table 1: *Physico-chemical properties of mordenite and mordenite nanocrystal zeolite*

Sample	S_{BET} (m^2/g)	Pore volume (cm^3/g) (micro)	Pore volume (cm^3/g) (total)	Si/Al ratio
mordenite	240	0.14	0.16	6
mordenite nanocrystal	379	0.16	0.208	15

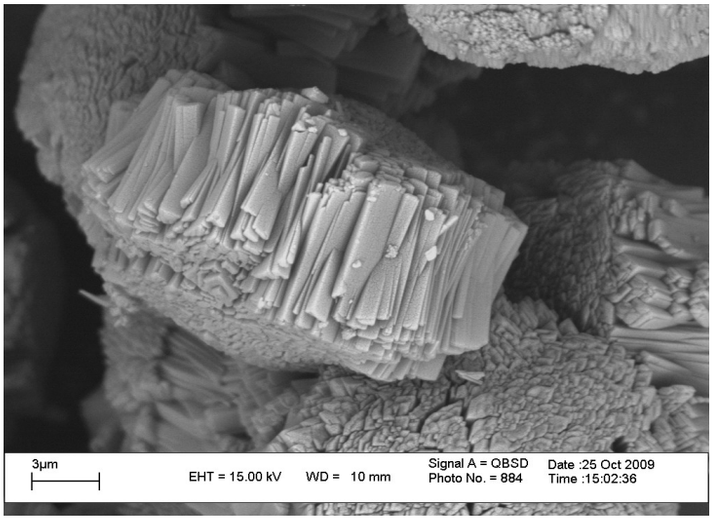

Figure 2: *Scanning Electron Microscopy (SEM) micrographs of mordenite nanocrystal.*

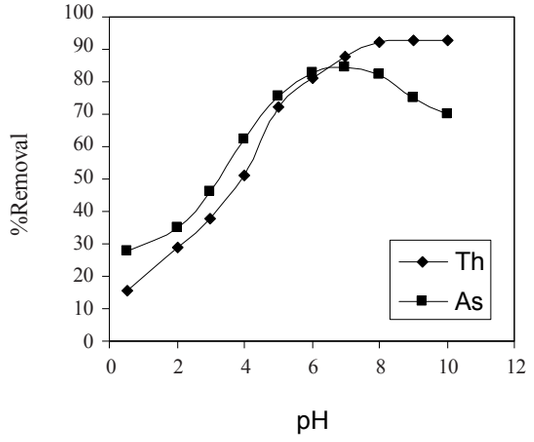

Figure 3: *Effect of solution pH on the metal ions removal by mordenite nanocrystals. Co=1.00 mM, mordenite dose=2g/l, sorption time=400 min.*

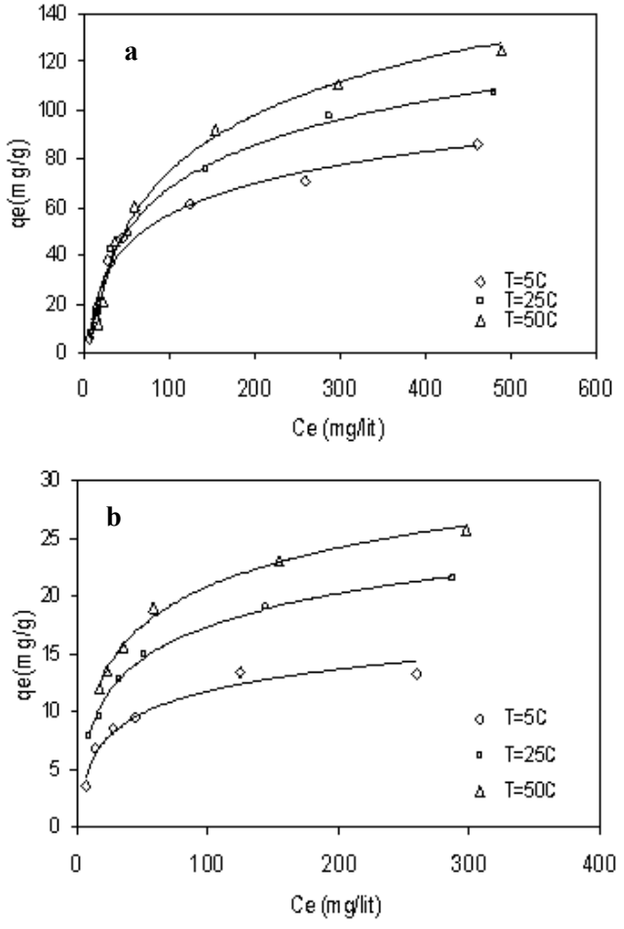

Figure 4: *Langmiure isotherms for removal of Tl(III)(a) and As(III) (b) at 5ºC (◊), 25ºC (□), 50ºC (Δ) by mordenite nanocrystal. Co=1.00 mM, dose=2g/l, adsorption pH was the optimal values for each ion uptake, sorption time=400 min.*

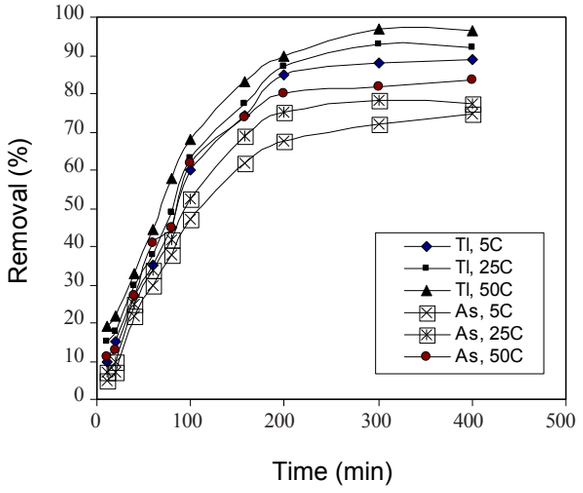

Figure 5: *Kinetics of Tl (III) and As (III) uptake by mordenite nanocrystal at 5ºC, 25ºC and 50ºC.Co=1.00 mM, dose=2g/l, at the optimal values of pH for removal viz 8.0 and 6.5 for Tl (III) and As (III) respectively.*

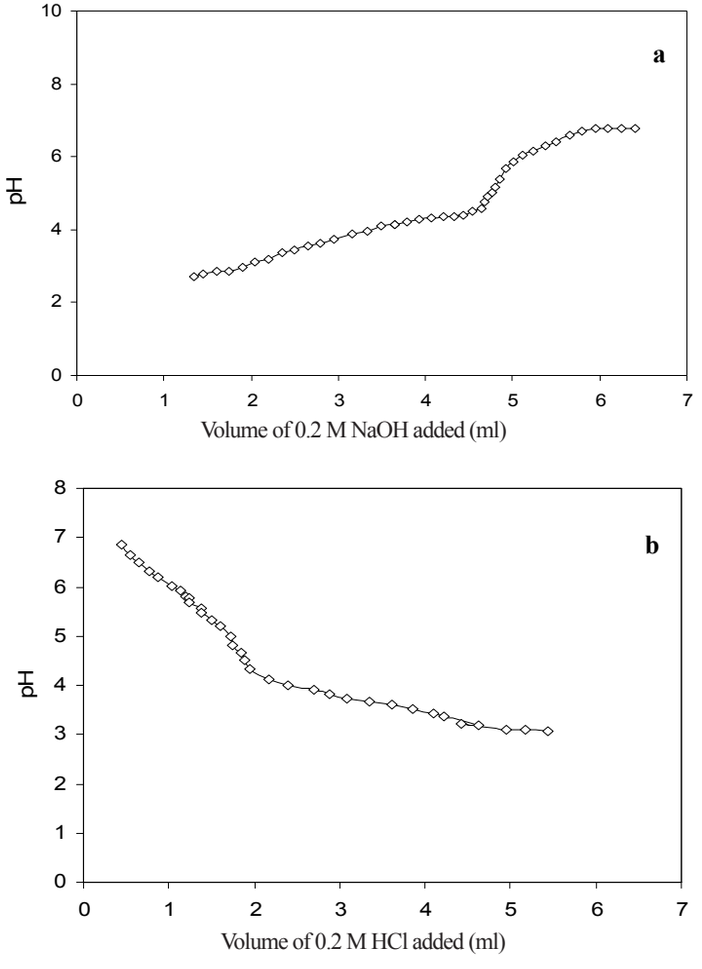

Figure 6: *Potentiometric titration curves of the treated mordenite nanocrystal with alkali (a) and acidic (b) agents.*

Table 2: *Langmiur and thermodynamic parameters for metal ions adsorption onto mordenite nanocrystal, Co=1.00 mM, dose=2g/l, sorption time=400 min, at the optimal values of pH for removal viz 8.0 and 6.5 for Tl(III) and As(III) respectively with using temperatures of 278, 298 and 323 K.*

	T (K)	Reference *Lemna minor*					
		Q_{max} (mmol/g)	K_L (1/mM)	$-\Delta G$ (kJ/ mol)	ΔH (kJ/mol)	ΔS (J/ mol K)	(R^+)
Tl^{3+}	278	0.627	0.896	1.863	11.236	38.1	0.9536
	298	0.766	1.020	1.426			
	323	0.836	1.563	0.864			
As^{3+}	278	0.563	0532	2.120	9.856	42.9	0.9852
	298	0.612	0.936	1.694			
	323	0.742	1.125	0.941			

[a] Obtained from Eq. (2) with R^2 >0.98.
[b] Obtained from Eq.(5) with $(R^2)^c$

Table 3: *Comparison between adsorption rate constants of the heavy metals, qe estimated and coefficients of correlation associated to the Lagergren pseudo-first-order and to the pseudo-second-order kinetic models at 278, 298 and 323 K.*

	T(K)	Pseudo-first order kinetic model			pseudo-second order kinetic model			$q_{e,exp}$ (mg/g)
		- $k_{1,ads}$($\times 10^{-3}$) (1/min)	$q_{e,cal}$	R^2 (mg/g)	$k_{2,ads}$ ($\times 10^{-3}$) (g/mg min)	$q_{e,cal}$	R^2 (mg/g)	
Tl^{3+}	278	5.13	35.74	0.723	3.42	70.02	0.958	71.52
	298	14.23	31.25	0.765	5.41	77.85	0.985	78.25
	323	19.83	24.96	0.837	8.64	84.63	0.995	85.32
As^3	278	8.63	14.25	0.811	5.23	12.56	0.998	13.52
	298	16.83	11.85	0.836	10.52	17.58	0.997	18.23
	323	24.58	5.74	0.825	11.85	20.01	0.996	20.58

Table 4: *The quantity of H^+ and OH^- of the mordenite nanocrystal structure after acidic and alkali treatment by the potentiometric titration data.*

pH	**$[H^+]_{total}$ (mmol/g)**	**$[OH^-]_{total}$(mmol/g)**
3	4.81	
9		1.73

3.1. Effect of pH

According to Figure 3, the optimal values of pH for removal are almost 8.0 and 6.5 for Tl (III) and As (III) respectively.

In pH 1–2, there is a balance reaction:

$$H^+ + HlC_4^- \rightarrow HTlCl_4$$

the main chemical species of thallium (III) is $HTlCl_4$ [21, 22], so the adsorption percentage of Tl (III) was lower.

In this pH also SiO_2 of Mordenite can be converted to H_2SiO_3 that it can be seemed as the demolition of the nano-structure.

However, at pH>5, with the increase of OH^- in solutions Cl^- in $TlCl_4^-$ was gradually replaced by OH^{-1}. And $[TlCl_2(H_2O)_3]^-$, $[Tl(H_2O)_4(OH)_2]^+$, $[Tl(H_2O)_5(OH)]^{2+}$ [23]

and so on, were formed in solutions, which is not favor of adsorption of thallium (III).

On the other hand because As^{3+} is stable at acidic pHs and AsO_3^{3-} is stable at alkali pHs, the decrease of pH decreases the As^{3+} removal only due to its effect on the nano-structure and not due to the As form. Also the probability of AsO_3^{3-} diffusion to nano-pores is less than As^{3+} with the more small size.

3.2. Adsorption isotherms in the batch reactors

Figures 4 (a-b) shows the obtained adsorption isotherms by mordenite nanocrystal at three different temperatures; 278, 298 and 323 K. According to Table 2, Q_{max} and K_L values were increased to remove heavy metal ions with increasing temperature. On the other hand, Q_{max} and K_L values for each metal ion uptake by Tl (III) were greater than those for As (III) at the same temperature. It also can be seen that the change of sorption temperature has a more effect on the shift and the slop of obtained sorption isotherms by the reference adsorbent, resulting on their Q_{max} and K_L values.

3.3. Thermodynamics study

The free energy change of the sorption reaction is given by

$$\Delta G = -RgT \ln K_L \quad (4)$$

According to the following equation:

$$\ln K_L = -\Delta G/R_gT = -\Delta H/R_gT + \Delta S/R_g \quad (5)$$

the plot of $\ln K_L$ as a function of 1/T (Van't Hoff plots) yields a straight line that ΔH and ΔS are found from the slop and intercept, respectively. R_g is the universal gas constant (8.314 J/mol K) and T is the absolute temperature (K).

As can be seen from Table 2, the negative values of ΔH confirms the endothermic character of sorption on mentioned metal ions-mordenite, whereas the low values of ΔS indicates that no remarkable changes on the entropy associated to the sorption process. The negative values of ΔG validate the feasibility of the sorption process, and the spontaneity of sorption. The sorption process of As (III) by mordenite nanocrystal was more spontaneity, but for Tl (III) was more endothermic than one.

3.4. Kinetic study and modeling

Figure 5 shows the changes of heavy metals removal with time in various temperatures that the experimental equilibrium adsorption ($q_{e,exp}$) can be determined from it. There have been several reports [22, 23] on the use of different kinetic models to adjust the experimental data of heavy metals adsorption on zeolite. With respect to the kinetic modeling, the first- and second-order kinetic models have been used.

The first-order rate expression of Lagergren considers that the rate of occupation of adsorption sites is proportional to the number of unoccupied sites. The linearized form of the pseudo first-order model is written as

$$\log (q_e - q) = \log q_e - (k_{1,ads}/2.303)\, t \quad (6)$$

where q_e and q (mg/g) are the amount of adsorbed heavy metals on the adsorbent at equilibrium and at the time t (min) and $k_{1,ads}$ (1/min) is the rate constant of the first-order sorption. Linear plots of

log (q_e-q) versus t indicate the applicability of this kinetic model [22]. However, to adjust Eq. (6) to the experimental data, the value of qe (equilibrium sorption capacity) must be pre estimated by extrapolating the experimental data to t=∞.

The Lagergren first-order rate constant ($k_{1,ads}$) and the equilibrium amount of metal removed (q_e) determined from the model are presented in Table 3 along with the corresponding correlation coefficient. However, the most important feature of this model is that it fails to estimate q_e. The linearized form of the pseudo-second-order model is written as:

$$t/q=1/(k_{2,ads}.\ q_e^2) + (1/q_e)\ t \quad (7)$$

Where $k_{2,ads}$ (g/mg min) is the rate constant of the second-order sorption. The plot t/q versus t should give a straight line if second-order kinetics are applicable and q_e and $k_{2,ads}$ can be determined from the slope and intercept of the plot, respectively.

Figure 6 shows the kinetic constants for the first and second-order rate modeling. It is important to notice that for the application of this model the experimental estimation of q_e is not necessary. Both parameters and the correspondent coefficients of correlation are also presented in Table 3. The correlation coefficients for the second-order kinetic model are equal to 0.997 and 0.999 for metal ions uptake by mordenite nanocrystal. The theoretical values of q_e also agree very well with the experimental ones. Both facts suggest that the sorption of these heavy metal ions follows the second-order kinetic models, which relies on the assumption that sorption, may be the rate limiting step. As can be seen from Table 3, according to the second-order kinetic model, the adsorbents with due attention to their $k_{2,ads}$ values to remove As (III) by mordenite nanocrystal were higher than it for Tl (III).

3.5. Potentiometric titration curves

From the potentiometric titration data (Figures 6a and b and Table 4), it is possible to make a qualitative and semi-quantitative determination of the nature and number of active sites present on the zeolite. The titration curves show the one inflection points at approximately pH 1.5-2.0 for acidic titration and at pH 4.5-5.0 for alkali titration. For pH values greater than the pKa, the sites are mainly in dissociated form and can exchange H^+ with metal ions in solution; while at pH values lower than pKa, complexation phenomenon can also occur [24].

The number of acidic sites and alkali sites per gram of mordenite nanocrystal (mmol/g) can be calculated by the estimation of inflection points (V_{eq}, ml) in the titration curves, using the following equations [25]:

$$[H^+]_{total}=V_{eq(NaOH)}\ .\ C_{NaOH}\ /\ m \quad (8)$$

and

$$[OH^-]_{total}=V_{eq(HCl)}\ .\ C_{HCl}\ /\ m \quad (9)$$

Where m (g) is the mass of mordenite nanocrystal.

Figures 6a and b and Table 4 show the potentiometric titration curves and $[H^+]_{total}$=4.81 mmol/g for treatment at pH 3 and $[OH^-]_{total}$=1.73 mmol/g for treatment at pH 9. So, the capacity of mordenite nanocrystal to uptake H^+ was more than it to uptake OH^- at these pHs. With attention to Figure 3, it can be seen the effect of H^+ uptake by mordenite nanocrystal on decreasing removal of Tl (III) and As (III) by mordenite.

4. CONCLUSIONS

On the base of the experimental results of this investigation, the following conclusions can be drawn:

1. Potentiometric titration can be used to study the pre-treatment process of adsorbent (mordenite nanocrstal) by acidic and alkali agents.
2. The Q_{max} and K_L values (Langmuir constants) to remove Tl(III) from the aqueous solution by mordenite nanocrystal were higher than those to remove As (III).

3. The thermodynamic studies showed that the sorption process of As (III) by mordenite nanocrystal was more spontaneity, but for Tl (III) was more endothermic than one.
4. The kinetic modeling showed that only the data corresponding to the first 25-35 min are adjusted approximately with pseudo-first-order model, since after this period the experimental data deviated considerably from those theoretical while these data were fitted well with pseudo-second-order kinetic models.

NOMENCLATURE

C_o	heavy metals initial concentration (mg/l)
C_e	heavy metals equilibrium concentration (mg/l)
q	adsorbed heavy metals on the adsorbent at time t (mg/g dry zeolite)
q_e	adsorbed heavy metals on the adsorbent at equilibrium (mg/g dry zeolite)
Q_{max}	Langmuir parameter, maximum adsorption capacity (mg/g dry zeolite)
K_L	Langmuir constant, sorption binding constant (l/mg)
V	suspension volume (l)
V_{eq}	consumed titrant volume to reach the inflection points
m	adsorbent dry weight (g)
R_g	universal gas constant (8.314 J/mol K)
T	absolute temperature (K)
ΔG	free energy change (kJ/mol)
ΔH	enthalpy change (kJ/mol)
ΔS	entropy change (J/mol K)
$k_{1,ads}$	rate constant of first-order sorption (1/min)
k_{2ads}	rate constant of second-order adsorption (g/g.min)

REFERENCES

1. R. M. Spearot, J. V. Peck, Waters, Environ. Prog. 3 (1984) 124-129.
2. T. H. Y. Tebbutt., Principles of water quality control. Fifth ed., Butterworth Heinemann, UK, 1998.
3. J. H. Choi, S. D. Kim, S.H. Noh, S. J. Oh, W. J. Kim, Microporous and Mesoporous Materials 87 (2006) 163–169
4. P. Liang, Y. C. Qin, B. Hu, C. X. Li, T. Y. Peng, Z. C. Jiang, J. Anal. Chem. 368 (2000) 638–640.
5. E. Maria Claesson, Albert P. Philipse, Colloids Surf. A: Physicochem. Eng. Asp. 297 (1–3) (2007) 46–54.
6. T. Sano, S. Wakabayashi, Y. Oumi, T. Uozumi, Micropor. Mesopor. Mater. 46 (2001) 67.
7. R. Dimitrova, G. Gündüz, M. Spassova, J. Mol. Catal. A Chem. 243 (1) (2006) 17–23.
8. T. C. Tsai, S. Y. Chang, I. Wang, Ind. Eng. Chem. Res. 42 (2003) 6053–6058.
9. F. Haimidi, R. Duartre, F. di Renzo, A. Bengueddach, F. Fajula, Morphological evolution of mordenite crystals. In: Proceedings of the 12th International Zeolite Conference, 3 (1999) 1803–1808
10. C. Shao, H. Y. Kim, X. Li, S. J. Park, D. R. Lee, Mater. Lett. 56 (2002) 24–29.
11. M. S. Sadjadi, A. Pourahmad, Sh. Sohrabnezhad, K. Zare, Mater. Lett., 61 (2007) 2923-2926.
12. Sh. Sohrabnezhad, A. Pourahmad, M. A. Sadjadi, M. A. Zanjanchi, Mater. Sci. Eng. C, 28 (2008) 202-205.
13. Sh. Sohrabnezhad, A. Pourahmad, M. S. Sadjadi, Mater. Lett., 61 (2007) 2311-2314.
14. I. Schmidt, C. Madsen, C. J. H. Jacobsen, Inorg. Chem. 39 (2000) 2279.
15. S. Mintova, V. Valtchev, Stud. Surf. Sci. Catal. 125 (1999) 141.

16. G. Zhu, S. Qiu, J. Yu, Y. Sakamoto, F. Xiao, R. Xu, O. Terasaki, Chem. Mater. 10 (1998) 1483.
17. B. O. Hincapie, L. J. Garces, Q. Zhang, A. Sacco, S. L. Suib, Micropor. Mesopor. Mater. 67 (2004) 19.
18. A. A. Shaikh, P. N. Joshi, N. E. Jacob, V. P. Shiralkar, Zeolites 13 (1993) 511.
19. M. M. J. Treacy and J. B. Higgins: Collection of Stimulated XRD Powder Patterns for zeolites, 4 th Ed. Elsevier, 243 (2001).
20. H. Robson (Ed.), Verified Syntheses of Zeolitic Materials. Second revised edition. Elsevier Science B. V., Amsterdam, 2001.
21. Z. Aksu, Separ. Purif. Technol. 21 (2001) 285–294.
22. B. Benguella, H. Benaissa, Water Res. 36 (2002) 2463– 2474.
23. F. Albert Cotton, F.R.S. Ceoffrey Wilkinson, Advanced Inorganic Chemistry, a Comprehensive Text, People Education Press, 1981, pp. 352–359.
24. T. A. Davis, B. Volesky, R.H.S.F. Vieira. Water Res, 34 (2000) 4270–4278.
25. A. Leusch, Z. R. Holan, B. Volesky. J Chem Technol Biotechnol 62 (1995) 279–88.